Ascorbic acid may not be involved in cryptochrome-based magnetoreception

Claus Nielsen[1,*], Daniel R. Kattnig[2], Emil Sjulstok[1], P. J. Hore[3], Ilia A. Solov'yov[1]

[1]Department of Physics, Chemistry and Pharmacy, University of Southern Denmark, Campusvej 55, DK-5230 Odense M, Denmark.

[2]Living Systems Institute and Department of Physics, University of Exeter, Stocker Road, Exeter, EX4 4QD, U.K.

[3]Department of Chemistry, University of Oxford, Physical & Theoretical Chemistry Laboratory, South Parks Road, Oxford OX1 3QZ, U.K.

*E-mail: clausnielsen@sdu.dk

Abstract

Seventeen years after it was originally suggested, the photoreceptor protein cryptochrome remains the most probable host for the radical pair intermediates that are thought to be the sensors in the avian magnetic compass. Although evidence in favour of this hypothesis is accumulating, the intracellular interaction partners of the sensory protein are still unknown. It has been suggested that ascorbate ions could interact with surface-exposed tryptophan radicals in photoactivated cryptochromes, and so lead to the formation of a radical pair comprised of the reduced form of the flavin adenine dinucleotide cofactor, $FAD^{\bullet-}$, and the ascorbate radical, $Asc^{\bullet-}$. This species could provide a more sensitive compass than a FAD-tryptophan radical pair. In this study of *Drosophila melanogaster* cryptochrome and *Erithacus rubecula* (European robin) cryptochrome 1a, we use molecular dynamics simulations to characterise the transient encounters of ascorbate ions with tryptophan radicals in cryptochrome in order to assess the likelihood of the [$FAD^{\bullet-}$ $Asc^{\bullet-}$]-pathway. It is shown that ascorbate ions are expected to bind near the tryptophan radicals for periods of a few nanoseconds. The rate at which these encounters happen is low, and it is therefore concluded that ascorbate ions are unlikely to be involved in magnetoreception if the ascorbate concentration is only on the order of 100 μM or less.

Introduction

The magnetic compass sense of migratory birds has attracted considerable attention over the last twenty years [1-6]. The proposal that a radical pair-based magnetic sensor is located in photoreceptor cells in the birds' retinas has emerged as the most likely mechanism to explain this remarkable phenomenon [1, 7]. The most promising molecular host for the radical pair intermediates is the protein cryptochrome [2, 3, 8], which contains a non-covalently bound flavin adenine dinucleotide (FAD) cofactor. Photoexcitation of the FAD followed by a series of fast intra-protein electron transfer reactions results in the formation of a flavin-tryptophan radical ion pair, [$FAD^{\bullet-}$ $W^{\bullet+}$]. The fate of this species, i.e. back electron transfer (recombination) or formation of a signalling state, is dictated by the coherent interconversion of the singlet and triplet states of the pair and the spin-selectivity of the recombination reaction. Through the electron Zeeman interaction this process can be sensitive to the direction and strength of the geomagnetic field [2].

Animal cryptochromes incorporate a chain of three or four tryptophan residues [3, 9, 10], shown in Fig. 1 and conventionally labelled, in order of increasing distance from the FAD, as W_A, W_B, W_C and W_D. Radical pairs involving FAD and either W_A or W_B have lifetimes of less than a nanosecond, which precludes sensitivity to the geomagnetic field [11]. [$FAD^{\bullet-}$ $W_C^{\bullet+}$] and [$FAD^{\bullet-}$ $W_D^{\bullet+}$], on the other hand, can persist for as long as microseconds [1, 12-14] – long enough to allow the yield of the signalling state to depend on the direction of an Earth-strength magnetic field. The identity of this long-lived form of the protein is uncertain; the assumption is that it passes on magnetic information via a conformational change in the C-terminal domain [15]. Although $FAD^{\bullet-}$ seems ideally suited to provide a strong directional response to the geomagnetic field, much of this advantage appears to be lost when it is combined with a tryptophan radical [16]. As a consequence, and in an attempt to account for some of the reported behavioural effects of weak radiofrequency fields, an alternative radical pair, [$FAD^{\bullet-}$ $Z^{\bullet}$], has been suggested [16]. Here, $Z^{\bullet}$ is a radical much simpler than $W^{\bullet+}$, one that has no significant internal magnetic (hyperfine) interactions. Currently the only biologically plausible $Z^{\bullet}$ radical is superoxide, $O_2^{\bullet-}$, but this can almost certainly be ruled out on the basis of its exceedingly fast spin relaxation [17]. The search for a biocompatible radical with a hyperfine structure that would afford large reaction anisotropies eventually led to the compromise proposal that, instead of $Z^{\bullet}$, the anion radical of ascorbic acid, $Asc^{\bullet-}$, could act as partner to the flavin semiquinone [16]. With only one large isotropic hyperfine interaction, a freely diffusing $Asc^{\bullet-}$ would be a more

favourable partner for $FAD^{\bullet-}$ than $W^{\bullet+}$. In this picture, the [$FAD^{\bullet-}$ $Asc^{\bullet-}$] radical pair would be formed from [$FAD^{\bullet-}$ $W^{\bullet+}$] by reduction of the tryptophan radical by ascorbate ions, $AscH^-$, followed by deprotonation of the neutral $AscH^{\bullet}$ radical. As W_C and W_D are located near the surface of the cryptochrome molecule, this electron transfer might occur rapidly compared to the singlet-triplet conversion in the [$FAD^{\bullet-}$ $W^{\bullet+}$] pair facilitated, for example, by direct interaction/complexation of the ascorbate ion with W_C or W_D. Note that as long as the ET is fast on the timescale of the spin evolution, the identity of the electron acceptor, i.e. $W_C^{\bullet+}$ or $W_D^{\bullet+}$, is immaterial. Ideally, [$FAD^{\bullet-}$ $Asc^{\bullet-}$] would be formed by static quenching, i.e. at a rate limited by electron transfer from $AscH^-$ to the tryptophan radical. Alternatively, if the resting state of the protein does not bind $AscH^-$ in the vicinity of $W_C^{\bullet+}$ or $W_D^{\bullet+}$, the electron transfer could still take place during diffusive encounters of $AscH^-$ with the surface-exposed tryptophan radical. This raises the question whether the encounter frequency could compete with spin relaxation in [$FAD^{\bullet-}$ $W^{\bullet+}$]. Presumably, either $AscH^-$ would need to be present at a high concentration or it would have to be funnelled towards the tryptophan radical, e.g. by electrostatic attraction, so as to enhance the reaction rate. With these possibilities in mind, we describe here an investigation of the efficiency of the proposed $AscH^- \rightarrow W^{\bullet+}$ electron transfer reaction in cryptochrome. In particular, we want to address whether ascorbate can bind to cryptochrome in the vicinity of W_C or W_D such that an efficient electron transfer reaction can take place. Note furthermore that vitamin C is abundant in the retina, where it is thought to serve as a component of the endogenous defence system that helps to limit UVB-induced, radical-related retinal damage [18]. The concentration of ascorbic acid in the retinas of guinea pigs and rats is about 1.6 mM [19, 20]; in human aqueous humour, it is present at a concentration of 1 mM [18].

No structures for any of the four avian cryptochromes have been determined. We have therefore focussed, in part, on *Drosophila melanogaster* cryptochrome (*Dm*Cry) for which a structure is available (PDB ID: 4GU5 [23, 24]). This protein has the fourth tryptophan, W_D, which could be important for magnetoreception [10]. In addition, we have studied a homology model of cryptochrome 1a from the migratory European robin (*Erithacus rubecula*, *Er*Cry1a). Although *Er*Cry1a has a fourth tryptophan, W_D, there is currently no experimental evidence for its involvement in electron transfer. Furthermore, as W_C and W_D are close to one another in the protein, and thus likely to react with $AscH^-$ at similar rates, and because the homology model may not be exact, we focus on the $W_C^{\bullet+}$ form of *Er*Cry1a.

Methods

Simulated systems

Our investigation of the interactions of $AscH^-$ with cryptochrome were based on all-atom molecular dynamics (MD) simulations performed using the NAMD package [25]. *Dm*Cry and *Er*Cry1a were investigated in three redox states: (i) the dark state (DS) that exists prior to the photo-induced charge separation, (ii) the light-induced [$FAD^{\bullet-}$ $W_C^{\bullet+}$] state (RPC), and (iii) the light-induced [$FAD^{\bullet-}$ $W_D^{\bullet+}$] state (RPD) [3, 9, 10, 21, 22] (Fig. 1). The simulation times are compiled in Table 1.

Short additional simulations

Additional MD runs were needed for the analysis of $AscH^-$ binding times. These simulations were repeated multiple times to provide better sampling statistics for determining the time ascorbate ions spend near W_C and W_D. The simulation times and number of replications are compiled in Table 2. All simulations were started from a configuration in which an ascorbate ion was within 5 Å of either W_C or W_D.

Homology model of *Er*Cry1a

A three-dimensional structure of *Er*Cry1a was built based on the amino acid sequence using the Swiss-model workspace [26-28]. Mouse cryptochrome 1 (PDB ID 4CT0 [29]) was used as a template for the homology model, covering 80% of the amino acid sequence with a similarity of 96%. As the crystal structure of the mouse cryptochrome does not include the flavin cofactor, an FAD molecule was placed inside the protein using the structure of *Arabidopsis thaliana* cryptochrome 1 (PDB ID 1U3C [30]) as a template, i.e. by superimposing the structure of the protein backbone with the backbone of the homology model of *Er*Cry1a. The homology model obtained in this way was equilibrated for 0.5 μs using the NAMD package [25]. The stability of the equilibrated structure was assessed in an additional 0.5 μs simulation, see Figure S1 in the Supplementary Information (SI).

MD simulation protocol

All simulations were carried out using the CHARMM36 force field [31-33] with CMAP corrections for proteins, along with earlier parameterizations for FAD and $FAD^{\bullet-}$ [11], which have been successfully employed in several MD studies

of cryptochrome [11, 34, 35]. A time step of 2 fs was used and the temperature was kept at 300 K using the Langevin thermostat. The pressure was held at 1 atm during the equilibration simulations, employing the Langevin barostat [36]. The SHAKE algorithm [37] was used to constrain bonds involving hydrogen atoms to fixed distances. Periodic boundary conditions were employed in all MD simulations and the particle-mesh Ewald (PME) summation method [38] was used to evaluate Coulomb forces. The van der Waals energy was calculated using a smooth cut-off of 12 Å with a switching distance of 10 Å.

The protein molecule and five ascorbate ions were solvated in a water box of dimensions 105 Å × 105 Å × 105 Å. This corresponds to a $AscH^-$ concentration of 7 mM. Na^+ ions were added to neutralize the system, and then additional Na^+ and Cl^- ions were added to achieve a NaCl concentration of 50 mM. Production simulations, see Table 1 and 2, were carried out in the canonical (*NVT*) ensemble.

The simulations followed a protocol comprising energy minimization, an equilibration phase, and the actual production run as specified in Table 1. During the energy minimization, the protein and FAD were constrained, such that only water molecules and ions could move. The equilibration phase was divided into three stages. First, the backbone of the protein was constrained by a strong harmonic potential for 1 ns. Next, a weaker harmonic constraint on the backbone was used for an additional 1 ns. Finally, a 2 ns equilibration without constraints was performed. The integration time step was set to 1 fs in all equilibration stages, which were carried out in the isothermal-isobaric (*NPT*) ensemble.

After these equilibration stages, five $AscH^-$ ions were added to the water box, far from the protein, and the water surrounding the ions was equilibrated: all atoms except water atoms within 16 Å of an $AscH^-$ were kept fixed during an initial energy minimization, followed by a 2 ns equilibration with harmonic constraints on the protein backbone. These steps were followed by additional 2 ns-runs without constraints in the *NPT* ensemble, in order to allow the box size to adapt to the added $AscH^-$ ions. All parameters were the same as in the previous equilibration runs. Analogous equilibration steps of this kind were performed for the simulations of the RPC and RPD states, i.e. the radical pair state of the solvated protein system was equilibrated before addition of the ascorbate ions.

Parameterizing ascorbate ions

There are no standard CHARMM force field parameters for ascorbate ions. We have derived them using the Force Field Toolkit (fftk) plugin in VMD [39, 40], in tandem with Gaussian09 quantum chemistry calculations [41]. Our approach for establishing the force field parameters for ascorbate strictly followed the official

fftk tutorial [39], consisting of geometry optimization, charge optimization, as well as optimization of bonded, angular and dihedral interactions. The obtained parameters are summarized in the SI.

Results

To quantify the possible interactions between ascorbate ions and cryptochrome, various analyses were performed. In particular, we explored the likelihood that ascorbate molecules approach the surface-exposed tryptophans of the triad or tetrad and searched for stable binding motifs to the cryptochrome surface and characterised their specificity.

The distance of closest approach

An important parameter that determines whether $AscH^-$ could react with tryptophan radicals in cryptochrome is the shortest distance between $AscH^-$ in solution and the sidechain of the tryptophan radical at the surface of the protein. This distance of closest approach was calculated as the smallest separation of the atomic coordinates of the reaction partners, including hydrogen atoms. Fig. 2 shows the time-dependence of the edge-to-edge distance of the closest of the five $AscH^-$ ions in the box to the tryptophans (W_C or $W_C^{\bullet+}$ and W_D or $W_D^{\bullet+}$) for the five different systems investigated (Table 1). Fig. 3 shows the related probability density function for the edge-to-edge distances. Figs 2 and 3 highlight different features of the same data. It should be noted, however, that a direct distance measurement could be misleading since periodic boundary conditions were used. Thus if the tryptophan is located near an edge of the simulation box, the closest $AscH^-$ might be located in the neighbouring periodic cell. Therefore the boundaries of the periodic cell were placed such that the tryptophan was at the centre of the cell before any distances were calculated.

Fig. 2 shows that in most instances $AscH^-$ ions do not bind close to the terminal tryptophans for times exceeding a few nanoseconds. (The two distance distributions and the distance trajectories are closely related due to the close vicinity of W_C and W_D; see Fig. 3). Instead, we mainly observed fleeting encounters during which the ions approach to distances of less than 10 Å, but diffuse apart within a few nanoseconds. For *Dm*Cry RPD (Fig. 2C) an ascorbate ion was bound for tens of nanoseconds at a distance of about 10 Å. A similar feature can be identified for *Dm*Cry RPC and *Dm*Cry DS (Figs 2B and 2A, respectively). This comparatively stable binding for a significant time is also visible in the probability density functions as a peak near 10 Å (Figs 3B and 3D). For *Er*Cry1a, a small peak at 5-7 Å (Figs 3A and 3C) hints at the presence of

weak binding modes of $AscH^-$ ions near $W_C^{\bullet+}$ (and thus W_D) in the RPC simulation. It is interesting to note that this binding mode, though weak, is peculiar to the radical pair state. The distributions in Fig. 3B and 3D also feature peaks at 15-20 Å, which suggest binding at remote sites. These sites are, however, too distant from the terminal tryptophans as to permit fast electron transfer reactions.

Binding times

It follows from Fig. 2 and the discussion above that ascorbate ions often approach the terminal tryptophans without staying bound for times significantly longer than a few nanoseconds. This does not necessarily mean that there is no binding, but hints at a rather weak interaction energy. In order to analyse these transient encounters in a quantitative way, we define the binding time as the time that an ascorbate ion spends within 10 Å of W_D or $W_D^{\bullet+}$, depending on the state of the protein. The choice of a 10 Å cut-off is prompted by Fig. 2. Since the number of observed binding events in the 200 ns long-time simulations is limited, a series of additional simulations was performed to determine the binding times with adequate sampling statistics (see Table 2 for details). In these short-time simulations the system was initiated in a "bound" state with an ascorbate-tryptophan (W_D) distance of approximately 5 Å, and the ascorbate ion was considered bound until it got more than 10 Å away from the tryptophan, at which point it was considered unbound for the rest of the simulation time. The total number of bound ascorbate ions at time *t* in all of the short-time simulations is shown in Fig. 4.

The ascorbate ions are attracted to the cryptochrome surface through electrostatic and van der Waals interactions. As the ascorbate ions are observed to associate with the terminal tryptophans for a short time, one can expect there to be an energy barrier that has to be overcome in order to leave the binding site, leading to a finite binding time, τ. Assuming first order kinetics and considering N_0 statistically independent simulations of $AscH^-$, the number of ascorbate ions bound at a time instant *t* is given by:

$$N(t) = N_0 \exp(-t/\tau) \ . \qquad (1)$$

Eq. (1) has been used to fit the simulation data shown in Fig. 4; the binding times, τ, are compiled in Table 3.

The results are consistent with those in Fig. 2. Typical brief binding events appear to last longer for *Dm*Cry than for *Er*Cry1a. This is also evident from the encounters just after 100 ns in Fig. 2A, 2C and 2E.

Cryptochrome surface electrostatics

It follows from Figs 2 and 3 that ascorbate ions occasionally approach the terminal tryptophan residues, even though persistent short-range binding does not occur. In order to further understand the characteristics of the ascorbate-protein interaction, we consider here the average electrostatic surface potential of the cryptochrome molecules calculated over the course of the simulations. Figs. 5 and 6 show this quantity for the DS and RPC states of *Dm*Cry and *Er*Cry1a. The difference between the electrostatic potentials of the two states is mainly attributable to the extra positive charge on $W_C^{\bullet+}$ in the radical pair state; only subtle differences result from the slightly different conformations of the two states of the proteins.

The electrostatic potential for *Dm*Cry is divided into two regions. The area near the terminal tryptophans is mainly positive, whereas a large part of the remaining surface shows a negative potential.

The electrostatic potential of *Er*Cry1a is fairly similar to that of *Dm*Cry, but is characterized by more irregularities resulting from regions of alternating potential. A significant difference is obvious right next to the terminal tryptophans, where the presence of the D321 residue in *Er*Cry1a results in a zone of negative potential. As expected, this effect is much less pronounced in the radical pair state, where the negative charge at D321 is partly compensated by the positive charge on the nearby $W_C^{\bullet+}$ radical.

Discussion

To determine whether ascorbate can react with radical pairs in cryptochrome, three questions need to be answered. First, does ascorbate ever get close to a tryptophan radical? Second, if it does, how long does it stay there? Third, does this encounter allow electron transfer to occur? The first question is addressed by Figs 2 and 3, which show that ascorbate occasionally approaches the tryptophan radicals on the surface of the cryptochrome molecule. The analysis of binding times (Fig. 4 and Table 3) suggests that encounters lasting more than a few nanoseconds are rare. Even if an ascorbate ion binds repeatedly, it is unlikely to remain in the vicinity of the terminal tryptophans for more than a few nanoseconds, as can be seen from Table 3, although longer binding times are possible (Fig. 2). Thus if the electron transfer from ascorbate to a tryptophan radical is relevant, it should occur in about 1 ns or less.

Whether these transient encounters allow an electron to be transferred from $AscH^-$ to one of the tryptophan radicals is determined by the intrinsic electron transfer rates which are mainly dictated by the free energy of the electron transfer

reaction. Based on the redox potentials for oxidation of tryptophan (to form the protonated tryptophan radical cation, E^0 = 1.15 V [42]) and reduction of the ascorbate ion (to form $AscH^{\bullet}$, E^0 = 0.72 V), we estimate a driving force of –0.43 eV for the reduction of $W^{\bullet+}$ by $AscH^-$ in aqueous solution. The reduction potential of $AscH^-$ was determined from a thermodynamic cycle using published values [43, 44] for the acid dissociation constants of $AscH^-$ (pK_a = 11.4) and $AscH^{\bullet}$ (pK_a = –0.45) and the reduction potential of $Asc^{\bullet}$ (E^0 = 0.015 V [45]). In combination with the solvation/binding energies calculated using a continuum electrostatic approach (see SI; non-polar contributions are expected to cancel to a good approximation), we estimate a driving force of –0.40 to –0.45 eV for the reaction of the protein-bound $W_D^{\bullet+}$ and $AscH^-$ in close vicinity (see the SI for details). Note that because both $AscH^-$ and $W_D^{\bullet+}$ are potential hydrogen donors, direct hydrogen atom transfer cannot provide an alternative to electron transfer, at least not until the indole nitrogen atom of $W_D^{\bullet+}$ has been deprotonated. Based on *in vitro* studies [8], this deprotonation occurs no faster than a microsecond, which is too slow for the ascorbate radical to be formed before appreciable spin dynamics and spin relaxation occur in [$FAD^{\bullet-}$ $W_D^{\bullet+}$]. As a consequence, direct electron transfer is the only viable reaction pathway and the only pathway discussed here.

Based on semi-empirical estimates of the electron transfer rate constant, such as the Rehm-Weller plot [46, 47] and the Moser-Dutton ruler [48], efficient electron transfer is anticipated for a driving force of –0.40 to –0.45 eV. In particular, the electron transfer reaction is estimated to correspond to the diffusion controlled plateau of the Rehm-Weller plot [46]. Furthermore, assuming a typical reorganization energy of 1 eV, electron transfer is estimated to proceed on a nanosecond timescale for an edge-to-edge separation of the redox centres of approximately 8 Å (estimate based on the Moser-Dutton expression [48]). Going beyond these rough estimates, we are interested in the comparatively slow electron transfer reaction at the protein surface or during the mutual approach of the reactants. This scenario is characterized by weak electronic coupling and the absence of appreciable solvent friction, i.e. it belongs to the domain of diabatic electron transfer [49]. In the Marcus normal region, which is applicable here, the intrinsic rate of electron transfer, $w(r)$, is given by [50, 51]

$$w(r) = \frac{2\pi}{h} V(r)^2 \frac{1}{\sqrt{4\pi\lambda(r)k_B T}} \exp\left(-\frac{\left(\Delta G_{et}(r) + \lambda(r)\right)^2}{4\lambda(r)k_B T} \right). \qquad (2)$$

While many of the pertinent parameters in Eq. (2) depend on distance (e.g. the reorganization energy, $\lambda(r)$, the driving force, $\Delta G_{et}(r)$, and the coupling matrix element, $V(r)$), the overall distance-dependence of $w(r)$ is dominated by $V(r)$, which decays exponentially [48-50] with the reaction distance, r. Thus, an exponential model of the form

$$w(r) = w_0 \exp(-\beta r) \tag{3}$$

should be applicable. Here, β is the characteristic decay length of $V(r)^2$ and w_0 is the reaction rate at the contact distance, which in the activation-less limit ($\Delta G_{et} = -\lambda$) is estimated to be $w_0 \approx$ 100-1000 ps^{-1} [46, 48]. For the relevant reaction here, $w_0 \approx$ 10-100 ps^{-1} is expected based on the estimated free energy of electron transfer and the reorganization energy [46, 48]. For electron transfer reactions in proteins, a typical value of the decay parameter is $\beta \approx 1.4$ Å^{-1}.

The relevance of the electron transfer reaction for the operation of cryptochrome as a magnetic compass sensor depends on whether the reaction is fast compared to the spin dynamics in the radical pair. To address this point, we need to evaluate the time-dependence of the charge transfer efficiency. As the reactant distance is constantly modulated by the relative diffusive motion of the ascorbate ion and the protein-bound tryptophan radical, this quantity cannot be assessed on the basis of a time-independent electron transfer rate (e.g. Eq. (2)) alone. Instead, a combined treatment of diffusion and reactivity is necessary. In general, this approach gives rise to a time-dependent rate coefficient, which accounts for the stochastic modulation of the reaction by the relative diffusive motion. In particular, it reflects the fact that after formation of the surface-exposed $W_D^{\bullet+}$ (or the less-exposed $W_C^{\bullet+}$), ensemble configurations with close-by ascorbate and protein molecules will react swiftly while those that are farther apart will react on a slower timescale. Unfortunately, a detailed analysis of this process requires a comprehensive description of the mutual diffusion (including specific binding interactions), which cannot be reconstructed from a limited set of MD trajectories. Instead we here model the survival probability of the tryptophan using the available MD samples.

We evaluated the probability that the primary radical pair survives for a time t_r in the presence of the $AscH^-$ molecules, each of which reacts with the tryptophan radical by an electron transfer reaction with the rate law given by

Eq (2). With typical radical pair lifetimes of several microseconds in mind and in agreement with the postulate that the spin evolution ought to proceed mainly in the secondary radical pair, [$FAD^{\bullet-}$ $Asc^{\bullet-}$], we have set t_r = 100 ns. The survival probability due to ascorbate ion *i* is given by

$$S_i(t_r) = \left\langle \exp\left(\int_{t_0}^{t_0+t_r} w\left(r_i(t)\right) \mathrm{d}t \right) \right\rangle , \tag{4}$$

with the angled brackets denoting an average over different realizations of the ensemble. t_0 is the moment of initiation of the electron transfer reaction. With the available data at hand, the ensemble average was approximated by trajectories representative of the primary radical pair, [$FAD^{\bullet-}$ $W^{\bullet+}$], averaged over t_0 (see SI for details). The survival probability of the primary radical pair in the presence of several (n_Q) ascorbate ions is

$$S(t_r) = \prod_{i=1}^{n_Q} S_i(t_r) . \tag{5}$$

For the majority of the MD simulations in this study, the above product comprises five ascorbate ions. The form of Eq. (5) suggests that the average survival probability due to a single $AscH^-$ ion could be introduced by

$$\bar{S}_1(t_r) = \sqrt[n_Q]{S(t_r)} . \tag{6}$$

Provided that the trajectories are statistically independent, this quantity affords a good estimate for the average reactivity of a single $AscH^-$ ion. This approach is expected to be approximately valid if the individual trajectories are characterized by brief encounters of ascorbate ions at the reactive site. We can therefore use Eq. (6) to evaluate the ascorbate concentration necessary to bring about electron transfer from ascorbate to the tryptophan radical with probability $p_r = 1 - S(t_r)$ within time t_r:

$$c = \frac{1}{N_A V} \frac{\log\left(1 - p_r\right)}{\log\left(\bar{S}_1\right)} , \tag{7}$$

where V is the volume of the MD box. Fig. 7 illustrates the ascorbate concentrations corresponding to a reaction probability of 90% within 100 ns as a function of w_0 for three different choices of β. Assuming that $w_0 \approx$ 10-100 ps^{-1}, this analysis suggests that ascorbate concentrations of approximately 0.1 mM and 10 mM are required for rapid reduction of $W_C^{\bullet+}$ in *Dm*Cry and in *Er*Cry1a, respectively. In *Er*Cry1a the required concentration is estimated to be high and largely independent of the intrinsic reaction rate, w_0, because the process is limited by the diffusive approach. On the other hand, the required concentration decreases with increasing w_0 for $W_C^{\bullet+}$ in *Dm*Cry, thereby indicating activation-control. For $W_D^{\bullet+}$ in *Dm*Cry a concentration of the order of 2 mM appears to be necessary as a consequence of the less efficient (compared to $W_C^{\bullet+}$) approach to the radical site. Because in *Dm*Cry, $W_C^{\bullet+}$ is swiftly reduced by the adjacent W_D (with formation of $W_D^{\bullet+}$) the comparatively high reactivity of $W_C^{\bullet+}$ with ascorbate probably does not provide an effective reaction pathway for the generation of [FAD$^{\bullet-}$ Asc$^{\bullet-}$]. Based on these estimates, we thus suggest that the charge transfer reaction from AscH$^-$ is probably inefficient and would require a very large local concentration of ascorbate, in particular for *Er*Cry1. Note that while the ascorbate can approach $W_C^{\bullet+}$ in *Er*Cry1a to shorter distances than in *Dm*Cry (see Fig. 3A), this is insufficient to yield a high electron transfer reactivity due to the low likelihood of these close encounters.

Conclusion

We have shown that the ascorbate anion, AscH$^-$, does not bind strongly to the dark state or the charge separated states of either *Dm*Cry or *Er*Cry1a. AscH$^-$ transiently encounters the surface-exposed tryptophan radicals of the [FAD$^{\bullet-}$ W$^{\bullet+}$] states with binding times of the order of nanoseconds. While these short encounters are in principle sufficient to facilitate electron transfer from AscH$^-$ to $W_D^{\bullet+}$, the infrequency of random encounters questions whether [FAD$^{\bullet-}$ Asc$^{\bullet-}$] could be an integral part of a magnetic compass sensor. In particular, without a dedicated binding motif, large concentrations of AscH$^-$, of the order of 10 mM, would be required to ensure that [FAD$^{\bullet-}$ Asc$^{\bullet-}$] is generated more rapidly than the loss of coherence in the [FAD$^{\bullet-}$ $W_D^{\bullet+}$] radical pair. Even though ascorbic acid can be considerably enriched in certain cell types [52], such high ascorbate concentrations are uncommon. The concentration of ascorbic acid in the retina is of the order of 1 mM [18-20]. For the radical pair involving $W_C^{\bullet+}$, our simulations indicate a higher reactivity to ascorbate. However, as $W_C^{\bullet+}$ rapidly converts W_D to $W_D^{\bullet+}$ this does not in general afford an efficient pathway for the

generation of [$FAD^{\bullet-}$ $Asc^{\bullet-}$].

While our calculations do not entirely rule out the possibility of electron transfer from external reductants, the reaction with $AscH^-$ at least does not appear to be favoured over random encounters of moderately reactive electron transfer partners. While it seems unlikely that $AscH^-$ plays a direct role in any magnetic sensing role of *Er*Cry1a, under physiological conditions the reduction of $W^{\bullet+}$ by $AscH^-$ could be involved in the regeneration of the dark state. It should be noted however, that since cryptochrome was simulated in water with ascorbate and NaCl, and therefore without interaction partners found *in vivo*, it is possible that binding of ascorbate near the surface-exposed tryptophan residues is stronger in the cellular environment.

Isothermal titration calorimetry could be used to determine the association constants for ascorbate binding to cryptochrome. The present study suggests that no significant binding should occur. Furthermore, magnetic field effects on *Dm*Cry could be measured in the absence and presence of ascorbate at sub-millimolar concentrations. According to the findings of this paper, no marked change of the field dependence of the action spectrum should become apparent (although the lifetime of the long-lived tryptophan radicals could be reduced in the presence of ascorbate).

The differences we find in $AscH^-$ binding times for *Dm*Cry and *Er*Cry1a could arise in part from inaccuracies in the homology model of *Er*Cry1a. Without an experimentally determined structure it is impossible to be sure of the reliability of the *Er*Cry1a model, but it is clear that errors in the structure could have a bearing on the estimated efficiency of electron transfer. Our results for *Dm*Cry, based on a high-resolution crystal structure, do not suffer from this problem.

Finally, Cry1a is just one of the four known avian cryptochromes and is therefore not the only candidate magnetoreceptor. Differences in sequence, structure and electron transfer properties could well make one of the other three (Cry1b, Cry2 and Cry4 [53]) more suitable as a detector of weak magnetic fields.

Acknowledgements

This work was supported by the European Research Council (under the European Union's 7th Framework Programme, FP7/2007–2013/ERC Grant 340451) and the US Air Force (USAF) Office of Scientific Research (Air Force Materiel Command, USAF Award FA9550-14-1-0095). IAS and CN are grateful to the Lundbeck Foundation for financial support. Computational resources for the simulations were provided by the DeiC National HPC Center, SDU.

Tables

Table 1: Summary of the long-time simulations. The simulation time does not include the equilibration steps.

System	State	Simulation time
*Dm*Cry	DS	200 ns
*Dm*Cry	RPC	200 ns
*Dm*Cry	RPD	200 ns
*Er*Cry1a	DS	200 ns
*Er*Cry1a	RPC	220 ns

Table 2: Summary of the short-time simulations.

System	State	Simulation time	Time Resolution	Replicas
*Er*Cry1a	RPC	5 ns	500 fs	250
*Dm*Cry	RPD	3.5 ns	500 fs	250

Table 3: Characteristic binding times, τ, of ascorbate ions determined by fitting the distribution of binding times from the short-time simulations (Fig. 4) using Eq. (1). R^2 is the coefficient of determination for the fits.

System	State	R^2	τ / ns
*Dm*Cry	RPD	0.992	1.45 ± 0.02
*Er*Cry1a	RPC	0.989	0.46 ± 0.01

Figures

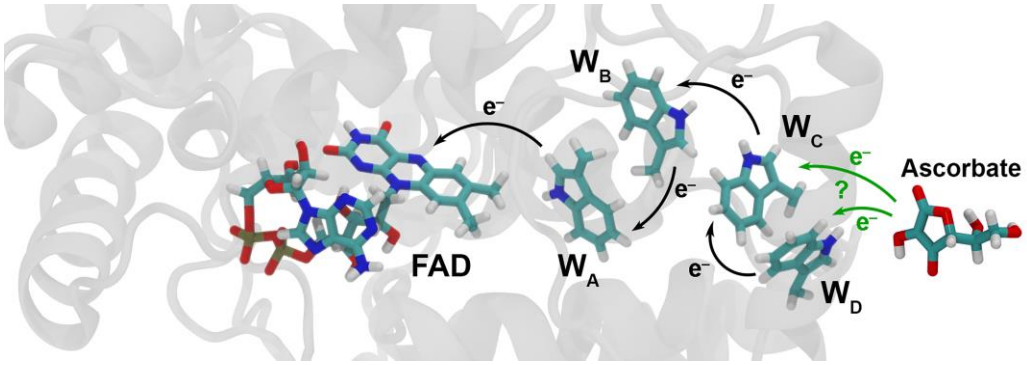

Figure 1: Cryptochrome electron transfer chain. Cryptochrome (in the background) contains a non-covalently bound FAD, which upon photo-excitation, FAD $\rightarrow$ FAD*, triggers a series of electron transfers within the protein: $W_A \rightarrow FAD^{*}$, $W_B \rightarrow W_A^{\bullet+}$, and $W_C \rightarrow W_B^{\bullet+}$, indicated with arrows. Here W_A, W_B, and W_C are three tryptophan residues, referred to as the tryptophan triad, which are conserved among different cryptochromes and different species [3, 21, 22]. In animal cryptochromes, a fourth electron transfer from W_D was recently discovered, $W_D \rightarrow W_C^{\bullet+}$ [9, 10]. The result is a radical pair consisting of the $FAD^{\bullet-}$ radical and either $W_C^{\bullet+}$ or $W_D^{\bullet+}$. $W_C^{\bullet+}$ and $W_D^{\bullet+}$ are located near the surface of the protein, potentially able to receive an electron from ascorbate ions ($AscH^{-}$), shown on the right. The protein displayed here is a homology model of cryptochrome 1a from the European robin, *Erithacus rubecula*.

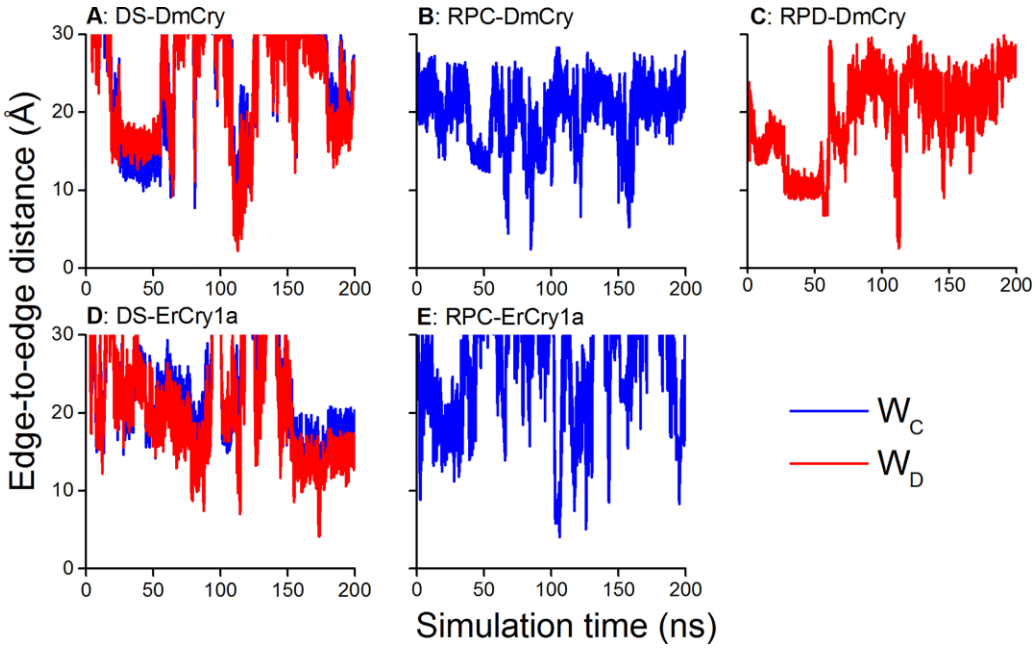

Figure 2: Edge-to-edge distances of terminal tryptophans and ascorbate ions. The figure shows the shortest distance from W_C and W_D to the nearest ascorbate ion ($AscH^-$) in the simulation box. Only the tryptophan in the radical state is considered in the radical pair state simulations. In **C** an $AscH^-$ ion resides at about 10 Å from $W_D^{\bullet+}$ for 30 ns, indicating a strong binding mode which is absent in the other simulations, except for a short period at around 120 ns in simulation **A,** where an $AscH^-$ closely approaches the tryptophans for several nanoseconds. Transient encounters of the terminal tryptophans and $AscH^-$ ions are observed in all the simulations, but rarely last for longer than a few nanoseconds.

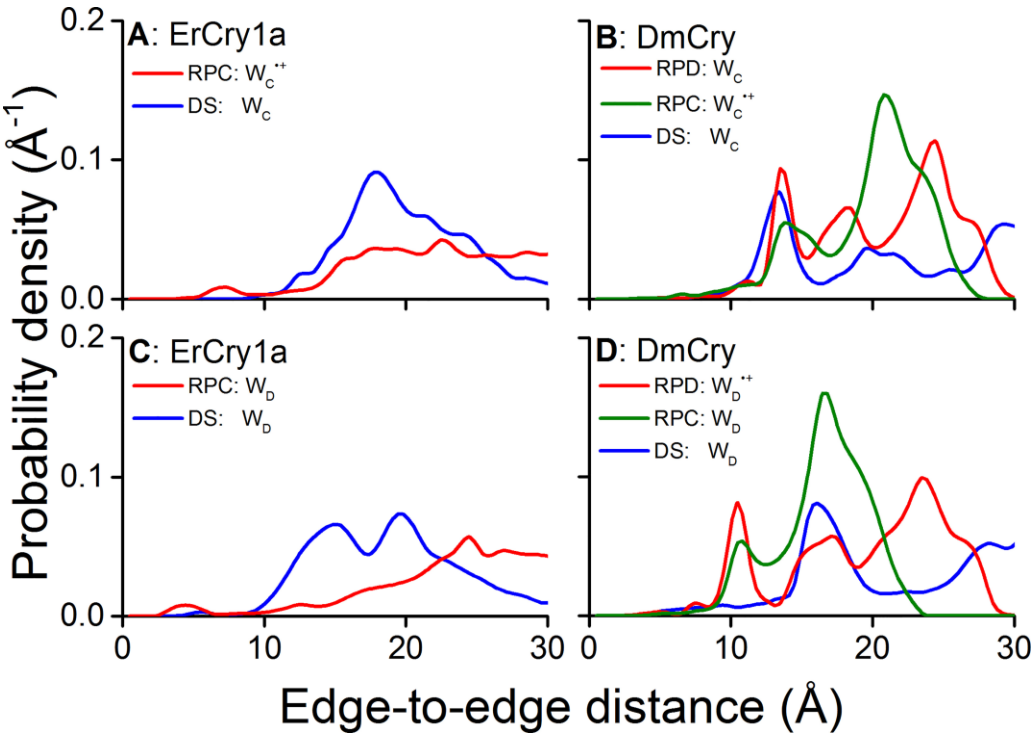

Figure 3: Edge-to-edge distances between tryptophans and ascorbate ions. The figure shows the probability density function for finding the closest ascorbate ion at a given edge-to-edge distance from the terminal tryptophans of *Er*Cry1a (*left*) or *Dm*Cry (*right*). The graphs for the two tryptophan residues are correlated because of their proximity in the protein. The distributions for the dark state of *Er*Cry1a in **A** and **C** show that the ascorbate ions seldom approach W_C and W_D closer than 10 Å. For the *Er*Cry1a RPC state the ascorbate ions are not found within 15 Å of $W_C^{\bullet+}$ except for brief encounters. For *Dm*Cry (**B** and **D**) a binding interaction stabilizes separations around 10 Å (as well as larger distances), but in general the ascorbate ions rarely get closer than 10 Å. In particular, no peak is observed for *Dm*Cry at small distances (~5 Å), unlike for *Er*Cry1a RPC.

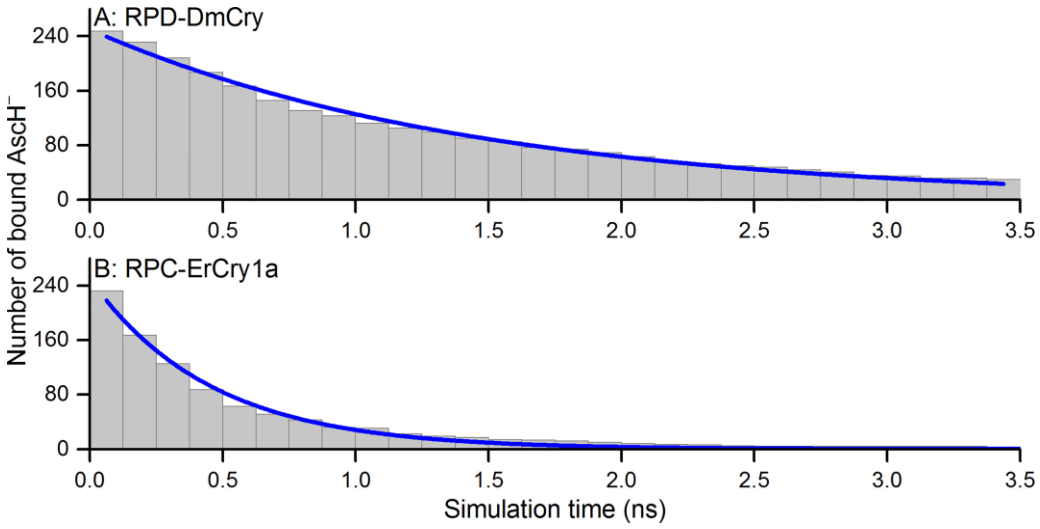

Figure 4: Ascorbate binding time determination. The number of bound ascorbate ions in *Dm*Cry RPD (**A**) and *Er*Cry1a RPC (**B**), as a function of time, have been evaluated from a series of short-time simulations starting from a bound configuration (simulation details summarized in Table 2). The binding time is defined as the time the ascorbate ion spends within 10 Å of W_D or $W_D^{\bullet+}$. Here, only times smaller than 3.5 ns have been considered. The time resolution of the simulation was 0.5 ps, and hence much smaller than the bin size in the histograms. The blue lines are fits based on Eq. (1). For *Dm*Cry the initial bound configuration had an edge-to-edge distance between $AscH^-$ and $W_C^{\bullet+}$ ($W_D^{\bullet+}$) of 4.52 Å (3.90 Å). For *Er*Cry1a the edge-to-edge distances were 4.28 Å and 5.44 Å, respectively.

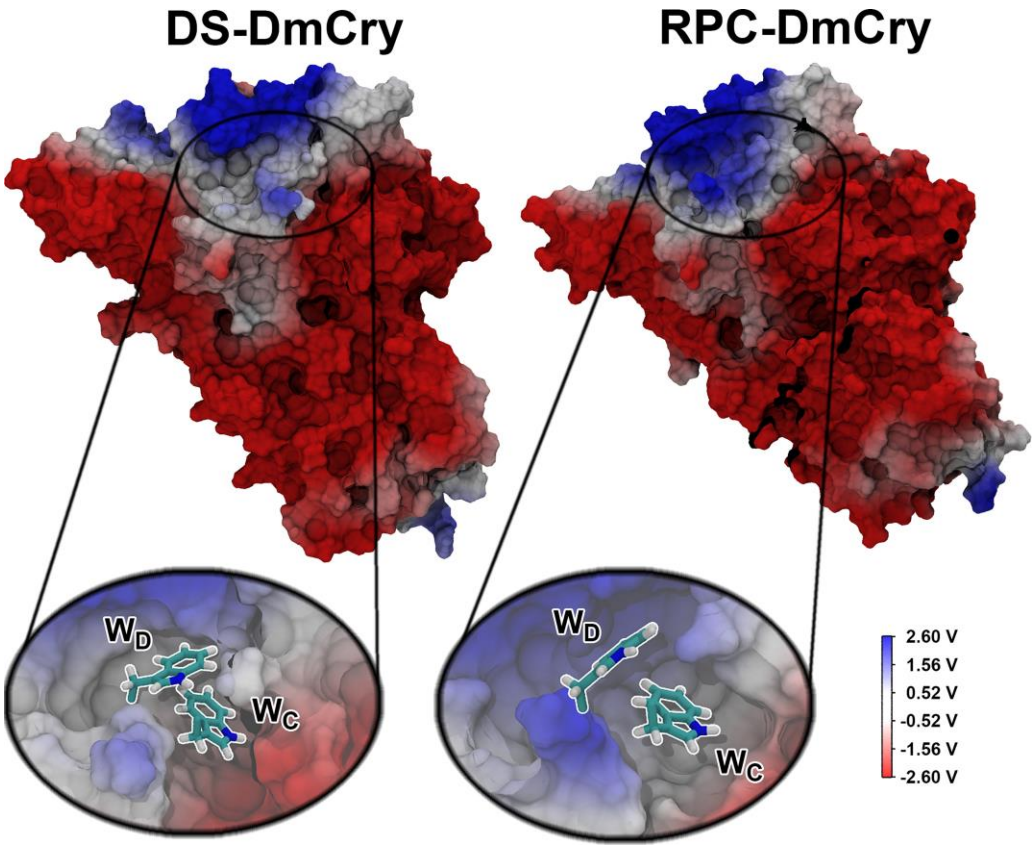

Figure 5: Surface electrostatic potential of *Dm*Cry. The electrostatic potential is positive (blue) near the tryptophans, in principle facilitating the approach of the negatively charged ascorbate ion. Most of the protein, however, has a negative potential (red). The average electrostatic potential was calculated as the mean value over 1000 snapshots evenly distributed over a 200 ns MD trajectory.

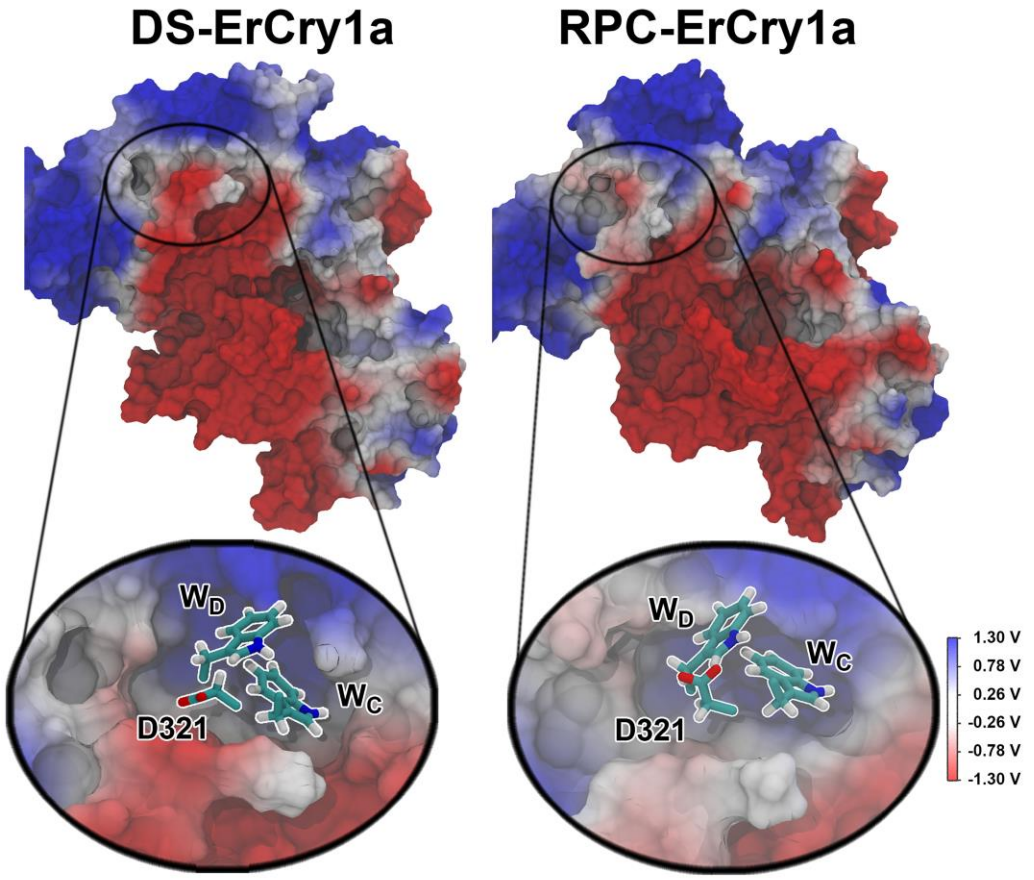

Figure 6: Surface electrostatic potential of *Er*Cry1a. Due to the negative charge at D321, the surface electrostatic potential is less positive in the vicinity of the terminal tryptophans than for *Dm*Cry. As in the case of *Dm*Cry, the protein exhibits a dominant negatively charged band. Here, the differences between the DS and RPC states are more pronounced. In particular, the negatively charged region at D321 is much less significant in the RPC state. The electrostatic potential was averaged over 1000 snapshots evenly distributed over a 200 ns MD trajectory.

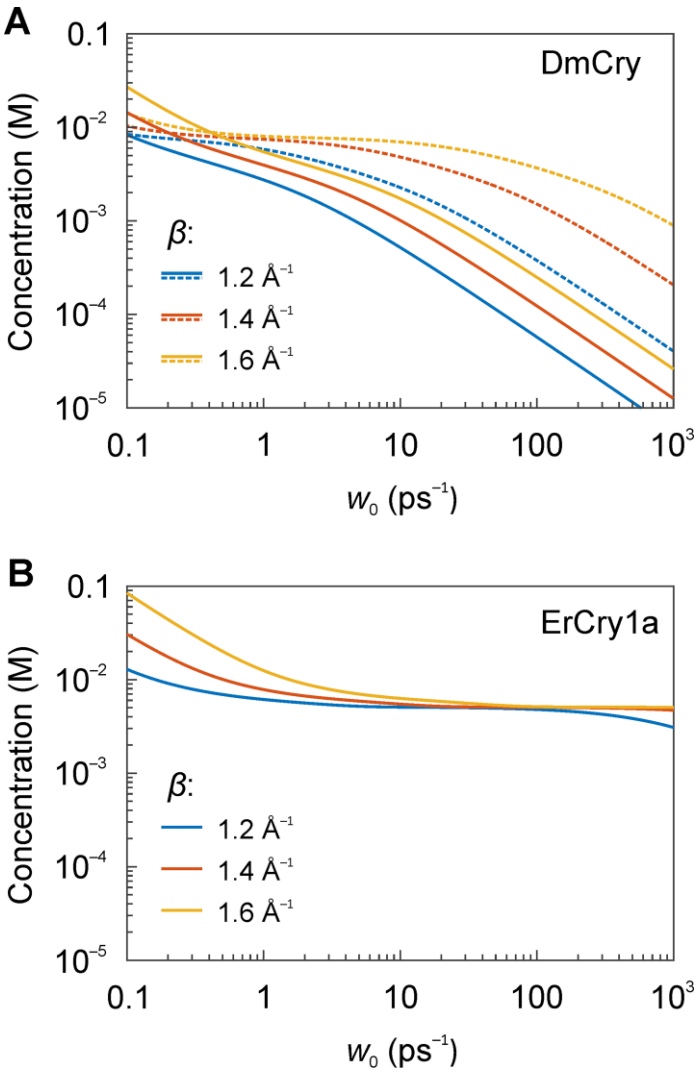

Figure 7: Ascorbate concentrations required for efficient quenching of the terminal tryptophan radicals. The figure shows the concentration of ascorbate, as calculated from Eq. (7), required to transform 90% of the [$FAD^{\bullet-}$ $W^{\bullet+}$] radical pairs to [$FAD^{\bullet-}$ $Asc^{\bullet-}$] within 100 ns. The plots give the required concentration as a function of the pre-exponential factor, w_0, in the electron transfer model given by Eq. (2) for three different values of the decay constant β. **A** applies to $W_C^{\bullet+}$ (solid lines) and $W_D^{\bullet+}$ (dashed lines) in *Dm*Cry; **B** is for $W_C^{\bullet+}$ in *Er*Cry1a (solid lines).

References

[1] Hore, P.J. & Mouritsen, H. 2016 The radical-pair mechanism of magnetoreception. *Annu. Rev. Biophys.* **45**, 299-344. (doi:10.1146/annurev-biophys-032116-094545).
[2] Ritz, T., Adem, S. & Schulten, K. 2000 A model for photoreceptor-based magnetoreception in birds. *Biophys. J.* **78**, 707-718. (doi:10.1016/S0006-3495(00)76629-X).
[3] Dodson, C.A., Hore, P.J. & Wallace, M.I. 2013 A radical sense of direction: signalling and mechanism in cryptochrome magnetoreception. *Trends Biochem. Sci.* **38**, 435-446. (doi:10.1016/j.tibs.2013.07.002).
[4] Wiltschko, W. 1968 Über den Einfluss statischer Magnetfelder auf die Zugorienteirung der Rotkehlchen (Erithacus rubecula). *Z. Tierpsychol.* **25**, 537-558.
[5] Wiltschko, W. & Merkel, F. 1966 Orientierung zugunruhiger Rotkehlchen im statischen Magnetfeld. *Verh. Dtsch. Zool. Ges.* **59**, 362-367.
[6] Wiltschko, W., Munro, U., Ford, H. & Wiltschko, R. 1993 Magnetic-inclination compass - a basis for the migratory orientation of birds in the northern and southern-hemisphere. *Experientia* **49**, 167-170. (doi:10.1007/Bf01989423).
[7] Maeda, K., Henbest, K.B., Cintolesi, F., Kuprov, I., Rodgers, C.T., Liddell, P.A., Gust, D., Timmel, C.R. & Hore, P.J. 2008 Chemical compass model of avian magnetoreception. *Nature* **453**, 387-390. (doi:10.1038/nature06834).
[8] Maeda, K., Robinson, A.J., Henbest, K.B., Hogben, H.J., Biskup, T., Ahmad, M., Schleicher, E., Weber, S., Timmel, C.R. & Hore, P.J. 2012 Magnetically sensitive light-induced reactions in cryptochrome are consistent with its proposed role as a magnetoreceptor. *Proc. Natl. Acad. Sci. U. S. A.* **109**, 4774-4779. (doi:10.1073/pnas.1118959109).
[9] Müller, P., Yamamoto, J., Martin, R., Iwai, S. & Brettel, K. 2015 Discovery and functional analysis of a 4th electron-transferring tryptophan conserved exclusively in animal cryptochromes and (6-4) photolyases. *Chem. Commun.* **51**, 15502-15505. (doi:10.1039/c5cc06276d).
[10] Nohr, D., Franz, S., Rodriguez, R., Paulus, B., Essen, L.O., Weber, S. & Schleicher, E. 2016 Extended electron-transfer in animal cryptochromes mediated by a tetrad of aromatic amino acids. *Biophys. J.* **111**, 301-311. (doi:10.1016/j.bpj.2016.06.009).
[11] Lüdemann, G., Solov'yov, I.A., Kubar, T. & Elstner, M. 2015 Solvent driving force ensures fast formation of a persistent and well-separated radical pair in plant cryptochrome. *J. Am. Chem. Soc.* **137**, 1147-1156. (doi:10.1021/ja510550g).
[12] Biskup, T., Hitomi, K., Getzoff, E.D., Krapf, S., Koslowski, T., Schleicher, E. & Weber, S. 2011 Unexpected electron transfer in cryptochrome identified by time-resolved epr spectroscopy. *Angew. Chem. Int. Ed.* **50**, 12647-12651. (doi:10.1002/anie.201104321).
[13] Biskup, T., Schleicher, E., Okafuji, A., Link, G., Hitomi, K., Getzoff, E.D.

& Weber, S. 2009 Direct observation of a photoinduced radical pair in a cryptochrome blue-light photoreceptor. *Angew. Chem. Int. Ed.* **48**, 404-407. (doi:10.1002/anie.200803102).
[14] Immeln, D., Weigel, A., Kottke, T. & Lustres, J.L.P. 2012 Primary events in the blue light sensor plant cryptochrome: Intraprotein electron and proton transfer revealed by femtosecond spectroscopy. *J. Am. Chem. Soc.* **134**, 12536-12546. (doi:10.1021/ja302121z).
[15] Chaves, I., Pokorny, R., Byrdin, M., Hoang, N., Ritz, T., Brettel, K., Essen, L.O., van der Horst, G.T., Batschauer, A. & Ahmad, M. 2011 The cryptochromes: blue light photoreceptors in plants and animals. *Annu. Rev. Plant Biol.* **62**, 335-364. (doi:10.1146/annurev-arplant-042110-103759).
[16] Lee, A.A., Lau, J.C.S., Hogben, H.J., Biskup, T., Kattnig, D.R. & Hore, P.J. 2014 Alternative radical pairs for cryptochrome-based magnetoreception. *J. R. Soc., Interface* **11**, 20131063. (doi:10.1098/Rsif.2013.1063).
[17] Hogben, H.J., Efimova, O., Wagner-Rundell, N., Timmel, C.R. & Hore, P.J. 2009 Possible involvement of superoxide and dioxygen with cryptochrome in avian magnetoreception: Origin of Zeeman resonances observed by *in vivo* EPR spectroscopy. *Chem. Phys. Lett.* **480**, 118-122. (doi:10.1016/j.cplett.2009.08.051).
[18] Tokuda, K., Zorumski, C.F. & Izumi, Y. 2007 Effects of ascorbic acid on UV light-mediated photoreceptor damage in isolated rat retina. *Exp. Eye Res.* **84**, 537-543. (doi:10.1016/j.exer.2006.11.005).
[19] Heath, H., Beck, T.C., Rutter, A.C. & Greaves, D.P. 1961 Biochemical changes in aphakia. *Vision Res.* **1**, 274-286. (doi:10.1016/0042-6989(61)90008-6).
[20] Woodford, B.J., Tso, M.O.M. & Lam, K.W. 1983 Reduced and oxidized ascorbates in guinea-pig retina under normal and light-exposed conditions. *Invest. Ophthalmol. Vis. Sci.* **24**, 862-867.
[21] Kavakli, I.H. & Sancar, A. 2004 Analysis of the role of intraprotein electron transfer in photoreactivation by DNA photolyase *in vivo*. *Biochem.* **43**, 15103-15110. (doi:10.1021/bi0478796).
[22] Sancar, A. 2003 Structure and function of DNA photolyase and cryptochrome blue-light photoreceptors. *Chem. Rev.* **103**, 2203-2237. (doi:10.1021/cr0204348).
[23] Zoltowski, B.D., Vaidya, A.T., Top, D., Widom, J., Young, M.W. & Crane, B.R. 2011 Structure of full-length *Drosophila* cryptochrome. *Nature* **480**, 396-399. (doi:10.1038/nature10618).
[24] Zoltowski, B.D., Vaidya, A.T., Top, D., Widom, J., Young, M.W. & Crane, B.R. 2013 Corrigendum: Structure of full-length *Drosophila* cryptochrome. *Nature* **496**, 252-252. (doi:10.1038/nature11994).
[25] Phillips, J.C., Braun, R., Wang, W., Gumbart, J., Tajkhorshid, E., Villa, E., Chipot, C., Skeel, R.D., Kale, L. & Schulten, K. 2005 Scalable molecular dynamics with NAMD. *J. Comput. Chem.* **26**, 1781-1802. (doi:10.1002/jcc.20289).
[26] Arnold, K., Bordoli, L., Kopp, J. & Schwede, T. 2006 The SWISS-MODEL

workspace: a web-based environment for protein structure homology modelling. *Bioinformatics* **22**, 195-201. (doi:10.1093/bioinformatics/bti770).
[27] Bordoli, L., Kiefer, F., Arnold, K., Benkert, P., Battey, J. & Schwede, T. 2009 Protein structure homology modeling using SWISS-MODEL workspace. *Nature Protocols* **4**, 1-13. (doi:10.1038/nprot.2008.197).
[28] Biasini, M., Bienert, S., Waterhouse, A., Arnold, K., Studer, G., Schmidt, T., Kiefer, F., Cassarino, T.G., Bertoni, M., Bordoli, L., et al. 2014 SWISS-MODEL: modelling protein tertiary and quaternary structure using evolutionary information. *Nucleic Acids Res.* **42**, 252-258. (doi:10.1093/nar/gku340).
[29] Schmalen, I., Reischl, S., Wallach, T., Klemz, R., Grudziecki, A., Prabu, J.R., Benda, C., Kramer, A. & Wolf, E. 2014 Interaction of circadian clock proteins CRY1 and PER2 is modulated by zinc binding and disulfide bond formation. *Cell* **157**, 1203-1215. (doi:10.1016/j.cell.2014.03.057).
[30] Brautigam, C.A., Smith, B.S., Ma, Z.Q., Palnitkar, M., Tomchick, D.R., Machius, M. & Deisenhofer, J. 2004 Structure of the photolyase-like domain of cryptochrome 1 from *Arabidopsis thaliana*. *Proc. Natl. Acad. Sci. U. S. A.* **101**, 12142-12147. (doi:10.1073/pnas.0404851101).
[31] Best, R.B., Zhu, X., Shim, J., Lopes, P.E.M., Mittal, J., Feig, M. & MacKerell, A.D. 2012 Optimization of the additive CHARMM all-atom protein force field targeting improved sampling of the backbone φ, ψ and side-chain χ_1 and χ_2 dihedral angles. *J. Chem. Theo. Comp.* **8**, 3257-3273. (doi:10.1021/ct300400x).
[32] MacKerell, A.D., Feig, M. & Brooks, C.L. 2004 Extending the treatment of backbone energetics in protein force fields: Limitations of gas-phase quantum mechanics in reproducing protein conformational distributions in molecular dynamics simulations. *J. Comput. Chem.* **25**, 1400-1415. (doi:10.1002/jcc.20065).
[33] MacKerell, A.D., Bashford, D., Bellott, M., Dunbrack, R.L., Evanseck, J.D., Field, M.J., Fischer, S., Gao, J., Guo, H., Ha, S., et al. 1998 All-atom empirical potential for molecular modeling and dynamics studies of proteins. *J. Phys. Chem. B* **102**, 3586-3616.
[34] Solov'yov, I.A., Domratcheva, T. & Schulten, K. 2014 Separation of photo-induced radical pair in cryptochrome to a functionally critical distance. *Sci. Rep.* **4**, 3845 (doi:10.1038/Srep03845).
[35] Sjulstok, E., Olsen, J.M.H. & Solov'yov, I.A. 2015 Quantifying electron transfer reactions in biological systems: what interactions play the major role? *Sci. Rep.* **5**, 18446. (doi:10.1038/Srep18446).
[36] Feller, S.E., Zhang, Y.H., Pastor, R.W. & Brooks, B.R. 1995 Constant-pressure molecular-dynamics simulation - the Langevin piston method. *J. Chem. Phys.* **103**, 4613-4621. (doi:10.1063/1.470648).
[37] Ryckaert, J.P., Ciccotti, G. & Berendsen, H.J.C. 1977 Numerical-integration of cartesian equations of motion of a system with constraints - molecular-dynamics of n-alkanes. *J. Comput. Phys.* **23**, 327-341. (doi:10.1016/0021-9991(77)90098-5).

[38] Darden, T., York, D. & Pedersen, L. 1993 Particle mesh ewald - an *n*.log(*n*) method for ewald sums in large systems. *J. Chem. Phys.* **98**, 10089-10092. (doi:10.1063/1.464397).
[39] Mayne, C.G., Saam, J., Schulten, K., Tajkhorshid, E. & Gumbart, J.C. 2013 Rapid parameterization of small molecules using the force field toolkit. *J. Comput. Chem.* **34**, 2757-2770. (doi:10.1002/jcc.23422).
[40] Humphrey, W., Dalke, A. & Schulten, K. 1996 VMD: Visual molecular dynamics. *J. Mol. Graph. Model.* **14**, 33-38. (doi:10.1016/0263-7855(96)00018-5).
[41] Frisch, M.J., Trucks, G.W., Schlegel, H.B., Scuseria, G.E., Robb, M.A., Cheeseman, J.R., Scalmani, G., Barone, V.G., Petersson, A., Nakatsuji, H., et al. 2013 Gaussian 09, Revision D.01. (Wallingford CT, Gaussian, Inc.
[42] Harriman, A. 1987 Further comments on the redox potentials of tryptophan and tyrosine. *J. Phys. Chem.* **91**, 6102-6104. (doi:10.1021/J100308a011).
[43] Khan, M.M.T. & Martell, A.E. 1967 Metal ion and metal chelate catalyzed oxidation of ascorbic acid by molecular oxygen. I. Cupric and ferric ion catalyzed oxidation. *J. Am. Chem. Soc.* **89**, 4176-4185. (doi:10.1021/Ja00992a036).
[44] Laroff, G.P., Fessende.Rw & Schuler, R.H. 1972 Electron-spin resonance spectra of radical intermediates in oxidation of ascorbic-acid and related substances. *J. Am. Chem. Soc.* **94**, 9062-9073. (doi:10.1021/Ja00781a013).
[45] Steenken, S. & Neta, P. 1979 Electron-transfer rates and equilibria between substituted phenoxide ions and phenoxyl radicals. *J. Phys. Chem.* **83**, 1134-1137. (doi:10.1021/J100472a005).
[46] Rehm, D. & Weller, A. 1969 Kinetics and mechanics of electron transfer during fluorescence quenching in acetonitrile. *Ber. Bunsenges. Phys. Chem.* **73**, 834-839.
[47] Rosspeintner, A., Kattnig, D.R., Angulo, G., Landgraf, S. & Grampp, G. 2008 The Rehm-Weller experiment in view of distant electron transfer. *Chem. Eur. J.* **14**, 6213-6221. (doi:10.1002/chem.200701841).
[48] Moser, C.C., Page, C.C., Farid, R. & Dutton, P.L. 1995 Biological electron-transfer. *J. Bioenerg. Biomembr.* **27**, 263-274. (doi:10.1007/Bf02110096).
[49] Gladkikh, V., Burshtein, A.I. & Rips, I. 2005 Variation of the resonant transfer rate when passing from nonadiabatic to adiabatic electron transfer. *J. Phys. Chem. A* **109**, 4983-4988. (doi:10.1021/jp044311y).
[50] Marcus, R.A. & Sutin, N. 1985 Electron transfers in chemistry and biology. *Biochim. Biophys. Acta* **811**, 265-322. (doi:10.1016/0304-4173(85)90014-X).
[51] Levich, V.G. 1965 In *Advances in Electrochemistry and Electrochemical Engineering* (eds. P. Delahay & C.W. Tobias), p. 249. New York Interscience.
[52] Bergsten, P., Amitai, G., Kehrl, J., Dhariwal, K.R., Klein, H.G. & Levine, M. 1990 Millimolar concentrations of ascorbic-acid in purified human mononuclear leukocytes - depletion and reaccumulation. *J. Biol. Chem.* **265**, 2584-2587.
[53] Liedvogel, M. & Mouritsen, H. 2010 Cryptochromes - a potential

magnetoreceptor: what do we know and what do we want to know? *J. R. Soc., Interface* **7**, S147-S162. (doi:10.1098/rsif.2009.0411.focus).